Science of the Total Environment 840 (2022) 156591

Contents lists available at ScienceDirect

Science of the Total Environment

journal homepage: www.elsevier.com/locate/scitotenv

Differential responses of bloom-forming *Ulva intestinalis* and economically important *Gracilariopsis lemaneiformis* to marine heatwaves under changing nitrate conditions

Meijia Jiang, Lin Gao, Ruiping Huang, Xin Lin, Guang Gao *

State Key Laboratory of Marine Environmental Science & College of Ocean and Earth Sciences, Xiamen University, Xiamen 361005, China

HIGHLIGHTS

- *Ulva* could survive heatwaves through shifting to micropropagules at lower nitrogen.
- *Ulva* could survive heatwaves by protecting its photosynthesis at higher nitrogen.
- *Gracilariopsis* died of bleaching under heatwaves regardless of nitrogen availability.

GRAPHICAL ABSTRACT

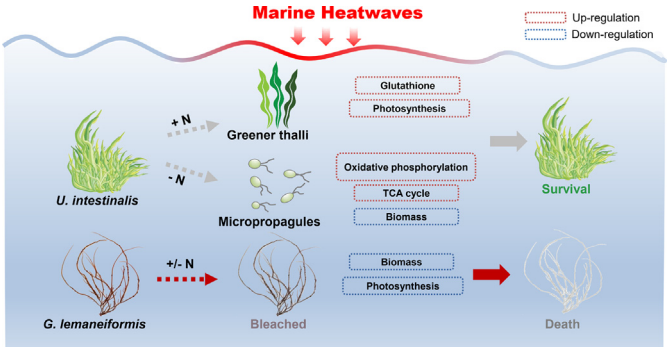

ARTICLE INFO

Editor: Julian Blasco

Keywords:
Green tides
Macroalgae
Marine heatwaves
Nitrogen
Photosynthesis
Seaweed cultivation

ABSTRACT

Marine heatwaves (MHWs) are affecting the survival of macroalgae. However, little is known regarding how the impacts of MHWs are regulated by nitrogen availability. In this study, we investigated the physiological and genetic responses of a green-tide macroalga *Ulva intestinalis* Linnaeus and a commercially cultivated macroalga *Gracilariopsis lemaneiformis* (Bory) E.Y. Dawson, Acleto & Foldvik under different nitrate conditions to simulated MHWs. Under nitrogen limited conditions (LN), heatwaves did not significantly affect biomass or *Fv/Fm* of *U. intestinalis* although it led to an earlier biomass decline due to more reproduction events, and meanwhile an upregulation in genes related to TCA cycle and oxidative phosphorylation was detected, supporting sporulation. Under nitrogen replete conditions (HN), heatwaves did not change biomass, *Fv/Fm* or photosynthetic pigments but reduced reproduction rate along with insignificant change of oxidative phosphorylation and TCA cycle related genes. Meanwhile, genes related to photosynthesis and glutathione metabolism were upregulated. Regarding *G. lemaneiformis*, heatwaves reduced its *Fv/Fm* and photosynthetic pigments content, leading to bleaching and death, and photosynthesis-related genes were also downregulated at LN. *Fv/Fm* was improved and photosynthesis-related genes were up-regulated by the combination of nitrogen enrichment and heatwaves, whereas *G. lemaneiformis* remained bleached and died by day 12. Therefore, *U. intestinalis* could survive heatwaves through shifting to micropropagules at LN and protecting its photosynthesis at HN. In contrast, *G. lemaneiformis* died of bleaching when suffering heatwaves regardless of nitrogen availability. These findings suggest that in future oceans with eutrophication and MHWs, the harmful alga *U. intestinalis* may have more advantages over the economic alga *G. lemaneiformis*.

* Corresponding author.
E-mail address: guang.gao@xmu.edu.cn (G. Gao).

http://dx.doi.org/10.1016/j.scitotenv.2022.156591
Received 1 March 2022; Received in revised form 7 May 2022; Accepted 6 June 2022
Available online 7 June 2022
0048-9697/© 2022 Elsevier B.V. All rights reserved.

1. Introduction

Marine heatwaves are considered to be prolonged extreme oceanic warm events for five or more days, which are warmer than the 90th percentile of average temperatures over the past 30 years (Hobday et al., 2016; Frölicher et al., 2018). Driven mainly by global warming, the global average duration and frequency of MHWs have increased by 17% and 34%, respectively, over the past 90 years (1925–2016) (Oliver et al., 2018). Furthermore, current climate models predict an increased MHWs intensity and duration in the future (Holbrook et al., 2020). MHWs were significantly correlated to the succession in the organisms, population and species levels, playing a crucial role in driving ecosystem structure (Oliver et al., 2019; Gao et al., 2021). For instance, MHWs cause coral bleaching and local extinction of mangrove and kelp forests, imposing negative impacts on invertebrates, fishes, seabirds and marine mammals (Smale, 2019; Feng et al., 2022). These events demonstrate the massive damage of MHWs to marine ecosystems.

Nitrogen as an essential component of numerous macromolecules, such as proteins, enzymes, nucleic acids, chlorophyll, etc., is considered as one of the most important environmental factors that influence physiological performance of algae (Gao et al., 2018a; Roleda and Hurd, 2019). In natural waters, nitrogen is usually the nutrient that most commonly limits growth of seaweeds (macroalgae) (Roleda and Hurd, 2019). Therefore, nitrogen enrichment usually stimulates photosynthesis and growth of seaweeds (Gao et al., 2018b; Traugott et al., 2020). In addition, previous studies have demonstrated that the resilience of seaweeds to environmental stress, such as ocean acidification and UVR, could be regulated by nitrogen availability in seawater (Cabello-Pasini et al., 2011; Gao et al., 2019). The nitrogen levels in coastal waters show a dramatic variation. It could be 6 μmol L^{-1} in the coastal waters in North Sea (Gao et al., 2017a) and be as high as 600 μmol L^{-1} in the pond where seaweeds were cultivated (Nelson et al., 2001), which may lead to differential responses of local seaweeds to environmental stress. Seaweeds are some of the most productive primary producers worldwide (Steneck et al., 2003). They supply basic materials and energy for other consumers, playing an essential role in nutrient cycle, sediment stabilization and carbon sequestration in coastal ecosystems (Krause-Jensen et al., 2016; Gouvêa et al., 2020). Kelp forests provide complex biogenic habitats for a range of other marine plants and animals (Sogard and Able, 1991), and are nurseries for a variety of juvenile fishes (Christie et al., 2009). The commercial value of macroalgae cannot be overlooked either, as they yield a range of commercially important products such as nutraceuticals, pharmaceuticals and food for humans and animals (Holdt and Kraan, 2011). However, the distribution, structure and productivity of seaweeds are under threat from MHWs over past years. MHWs have caused localized mortality events and substantial loss of canopy seaweeds (Smale et al., 2013; Wernberg et al., 2016; Thomsen et al., 2019). Between 2014 and 2016, extreme MHWs resulted in unprecedented losses of Bull kelp (*Nereocystis luetkeana*) forests along 350 km of coastline in northern California, and the previous extensive giant kelp forests have not recovered till now (McPherson et al., 2021). Meanwhile, some species are showing opposite responses to MHWs. The recruitment of the invasive kelp *Undaria pinnatifida* and green *Ulva* spp. in the South Island of New Zealand was promoted by MHWs (Thomsen et al., 2019). Furthermore, simulated summer MHWs hindered the growth rates of native seaweeds (*Fucus serratus* and *Chondrus crispus*) while promoted the growth of *Sargassum muticum* (Gao et al., 2021). Thus, different species of macroalgae and their fate will be affected differently by marine heatwaves.

Ulva species have become the problematic agents of global green tide events (Smetacek and Zingone, 2013) due to their fast growth rates and robust capacities to acclimate to environmental changes (Gao et al., 2017a). Massive green macroalgal blooms have occurred in Europe (Denmark, the Netherlands, France and the UK), Asia (China, Japan and Korea), North America and Australia (Choi et al., 2010; Kim and Se-Kwon, 2011). Since 2007, *Ulva* blooms have occurred continuously along the Yellow Sea coast and erupted every spring for the next 15 years. The average distribution area and the cover area of green tides in China were reported to be 37,000 km^2 and 450 km^2, respectively, which caused huge economic losses to the local government (Wang and Wu, 2021). *Ulva* negatively affects coastal ecosystems via rapidly expanding and depleting oxygen in the water column and benthic environment when decomposing (Lomstein et al., 2006). Green tides can also interfere with coastal nitrogen and carbon cycles and microplastic distribution (Zhang et al., 2019; Feng et al., 2020).

The genus *Gracilarioids* is distributed worldwide, from the equator to high latitudes (Oliveira and Ragan, 1994). In the 1970s, Ryther and coworkers demonstrated that species of *Gracilarioids* are some of the most productive algae in the world for their capacity to achieve high yields while producing commercially precious extracts (Capo et al., 1999). Up till now, as an important source of agar extracted worldwide, *Gracilarioids* is of great economic importance (Sambhwani et al., 2022). It is widely cultivated in Japan, Southeast Asia, Hawaii and the Caribbean, which is used in a variety of applications including food, medicine and cosmetics (Torres et al., 2019). In China, *Gracilarioids* production reached 348,085 tons (dry weight), and the area under cultivation was 9388 ha in 2019 (China Fishery Statistical Yearbook, 2020).

Although there are some studies that demonstrate the impacts of MHWs on macroalgae, our understanding on how MHWs affect bloom-forming and economically important macroalgae is still scarce particularly combined with nitrogen availability. We hypothesize that increased nitrogen availability can alleviate the negative effects of MHWs on macroalgae since nitrogen is one of the most important factors regulating responses of macroalgae to environmental stress (Werner et al., 2016; Gouvêa et al., 2017). In this study, *Ulva intestinalis* Linnaeus and *Gracilariopsis lemaneiformis* (Bory) E.Y. Dawson, Acleto & Foldvik are chosen to test this hypothesis and investigate the combined effects of MHWs and nitrogen on bloom-forming and economically important macroalgae.

2. Materials and methods

2.1. Seaweeds collection and identification

Around 100 g of *U. intestinalis* Linnaeus and 200 g of *G. lemaneiformis* (Bory) E.Y. Dawson, Acleto & Foldvik were respectively collected from the intertidal reaches of Xiamen (118.04°E, 24.26°N) and the seaweed farm of Ningde (119.31°E, 26.39°N), Fujian province of China in April 2021. The seawater temperatures at sampling locations were 19.7 °C for Xiamen and 19.2 °C for Ningde. The in situ nutrient levels were 5 μmol L^{-1} nitrate and 0.3 μmol L^{-1} phosphate for Xiamen, and 23 μmol L^{-1} nitrate and 1.5 μmol L^{-1} phosphate for Ningde. The daily light doses that seaweeds could receive were 0.9 MJ m^{-2} for Xiamen and 0.8 MJ m^{-2} for Ningde.

The plants were haphazardly selected and delivered to the lab in a cool container (4–6 °C). Debris and epiphytes were gently removed with filtered natural seawater.

Before the experiment, two species of macroalgae were both preincubated for one month at 20 ± 1 °C with an irradiance of 80 μmol photons m^{-2} s^{-1} and a 12 h:12 h (light/dark) cycle. The temperature and light dose were close to the conditions at the sampling site. ITS sequence of *U. intestinalis* was retrieved from GenBank and compared to the sequences obtained in the present study. To search for highly similar sequences in the National Center for Biotechnology Information (NCBI) database, BLAST (Basic Local Alignment Search Tool, http://ncbi.nlm.nih.gov/blast) was used to analyze the nucleotide sequences. *Ulva intestinalis* clone 6XM-1 KT802949.1 was found to be highly matched (99.69%) to the *Ulva* species used in this study. The nucleotide sequence of *U. intestinalis* in this study was uploaded to GenBank with the accession number of ON350969.

2.2. Heatwaves scenarios

The MHW definition given by Hobday et al. (2016) was used in this study: a heatwave is described as an exceedance of the 90th percentile of the region's seasonal temperature, for at least 5 consecutive days.

Heatwaves scenarios were created using regional data and current classifications (Li et al., 2019; Yao et al., 2020). As such, the 'control' ambient temperature (20 °C) and 'heatwave' temperature (23 °C) were identified to test the effects of heatwaves on the physiological response of two macroalgae. The study ran for 4 weeks (Nepper-Davidsen et al., 2019). On day 0, the temperature was kept at the same level as the previous day (20 °C). From days 1 to 6, the temperature within each heatwave system was increased by 0.5 °C per day (Winters et al., 2011) until the experimental temperature (23 °C) had been achieved (temperature-rising period). Once the experimental temperature was achieved, heatwaves were maintained until day 12 (7 days in total, temperature-maintaining period). From days 13 to 18, temperatures were reduced at a rate of 0.5 °C per day until control temperature was reached (temperature-decreasing period). At the end of the heatwaves treatment, the macroalgae were left to recover for a week (7 days in total, recovery period). For the culture of *G. lemaneiformis*, it was ended by day 12 because heatwaves treatments led to the bleaching and complete death of thalli.

2.3. Experimental design

After one month of acclimation period at 20 °C with the last week of nitrogen-limited incubation using natural seawater, eleven *U. intestinalis* fronds of 10 cm in length were selected and placed into 1 L polycarbonate flasks (0.6 g L^{-1}), each filled with 1 L of filtered natural seawater. The thalli were cultured under the treatment conditions in combinations of two temperature (20, 23 °C; coded as HW^- and HW^+, respectively) and nitrate (8, 200 μmol L^{-1}; coded as low nitrate, LN and high nitrate, HN respectively) levels. Under nitrate-limited and replete conditions, the effects of heatwaves were investigated using a fully crossed factorial design. The nitrate concentration of natural seawater (8 μmol L^{-1}) and temperature (20 °C) were set as the control condition. The phosphorus concentration was set as 50 μmol L^{-1} to obviate phosphorus limitation. Three replicate flasks were run for each treatment. The light intensities (80 μmol photons m^{-2} s^{-1}) with a photoperiod of 12 h:12 h (light/dark) were set via intelligent illumination incubators. Flasks were shaken twice every day and seawater was renewed every 3 days. Same experimental design was used for *G. lemaneiformis* (1 g L^{-1}).

2.4. Measurement of biomass and chlorophyll fluorescence of photosystem II (PSII)

After removing surface water by gently blotting the fronds with tissue paper, the fresh weight was determined by weighing using a balance (BSA124S, Sartorius, Germany) every 2 days (Li et al., 2019). When recording fresh weight, the removed biomass for different analyses (e.g. *Fv/Fm*; pigment content; RNA extraction) was considered. As an effective indicator, the maximal photochemical efficiency of PSII (*Fv/Fm*) can reflect the physiological status and photosynthetic activity of algae exposed to environmental stressors (Tan et al., 2019). Therefore, *Fv/Fm* of *U. intestinalis* and *G. lemaneiformis* was measured with a pulse amplitude modulation (PAM) fluorometer (MC-PAM, Walz, Germany) on days 0, 6, 12, 18 and 24 during the experiment. The saturating pulse was set to 2500 μmol photons m^{-2} s^{-1} (10 s). Before each measurement, a sample of 2–3 cm in length was randomly cut from every flask to measure. To ensure that all PSII reaction centers were fully oxidized, samples of macroalgae were dark-acclimated for 20 min for all measurements (Li et al., 2019).

2.5. Pigments content

Approximately 50 mg of fresh weight fronds were collected every 6 days and frozen at −20 °C until extraction. To assess the contents of chlorophyll *a* (Chl *a*), chlorophyll *b* (Chl *b*) and carotenoids, samples were extracted in 2 mL 95% ethanol at 4 °C for 24 h in darkness. Contents of pigments were estimated according to Alan and Wellburn (1994). The contents of Chl *a*, Chl *b* and carotenoids (mg·g^{-1} FW) were determined by the following equations:

$$\text{Chl } a = 13.36 \times A_{665} - 5.19 \times A_{649}$$

$$\text{Chl } b = 27.43 \times A_{649} - 8.12 \times A_{665}$$

$$\text{Carotenoids} = (1000 \times \text{A470} - 2.05 \times \text{Chl } a - 114.8 \times \text{Chl } b)/245$$

The content of phycobiliprotein, phycoerythrin (PE), was determined according to (Beer and Eshel 1985). Samples were disrupted by grinding with a metal grinder and extracted in 0.1 M PBS buffer, pH 6.8. The extract was centrifuged and the absorbance of these extracts was measured at 455, 564 and 592 nm with an ultraviolet-visible spectrophotometer (TU-1810DASPC, PERSEE, China) to calculate PE content. The content of PE (mg·g^{-1} FW) was determined by the following equation:

$$\text{PE} = [(A_{564} - A_{592}) - (A_{455} - A_{592}) \times 0.2] \times 0.12$$

2.6. Reproduction rate

Reproductive behaviors of *U. intestinalis* were accompanied by color transformation and gametophytes release (Gao et al., 2017b). All these transformations were verified by microscopy. Vegetative cells were green initially, containing several granular chloroplasts. Pyriform gametes were formed within the sporangia and subsequently liberated from the sporangia. After discharging all gametes, the cells become empty. The thalli transferred from green to yellow, and finally appeared white (Fig. 1). Tetrasporophyte of *G. lemaneiformis* was used in this study and tetraspore release had been found before this experiment (Fig. S1). The monitoring of reproductive feature of *G. lemaneiformis* was based on Ye et al. (2006) and Mi et al. (2017). The samples were checked daily. No reproduction events were observed for *G. lemaneiformis* during the culture period (Fig. S2). The ratio of individuals showing reproduction to the total individuals was calculated as reproduction rate.

2.7. RNA extraction and cDNA libraries preparation

One hundred milligrams fresh samples of *U. intestinalis* (cultivated for 7 and 24 days) and *G. lemaneiformis* (cultivated for 6 days) were harvested from each flask and dried with tissue paper. The *G. lemaneiformis* under the heatwaves treatment began to die on day 12 and no samples were taken at this time given possible RNA degradation. Each treatment included three replicates. All these samples were frozen in liquid nitrogen, and stored at −80 °C. Samples were sent to BGI Genomic Center (Shenzhen, China) where RNA was extracted, purified and checked. Total RNA meeting quality standards was used to construct cDNA libraries through processes such as RNA purification, mRNA isolation and fragmentation, double-stranded cDNA synthesis, adapter ligation and enrichment (Peredo and Cardon, 2020). The constructed cDNA libraries were tested using an Agilent 2100 Bioanalyzer and then sequenced using the Illumina HiSeq™ 4000 platform (Radecker et al., 2021).

2.8. De novo assembly and unigene annotation

After low-quality sequences were filtered out from raw reads obtained by sequencing, adaptor sequences, fuzzy data, and clean reads were de novo assembled by Trinity v2.0.6 and the transcripts were cluster into unigenes by TGICL v2.0.6. Bowtie2 v2.2.5 was used to map the clean reads to unigenes (Langmead and Salzberg, 2012), and the gene expression levels were calculated with RSEM v1.2.8 (Dewey and Li, 2011).

The unigenes were aligned and annotated by the Basic Local Alignment Search Tool (BLAST) v2.2.23 with the non-redundant nucleotide sequences (NT), non-redundant protein sequences (NR), Kyoto Encyclopedia of Genes and Genomes (KEGG), Cluster of Orthologous Groups of proteins (COG)

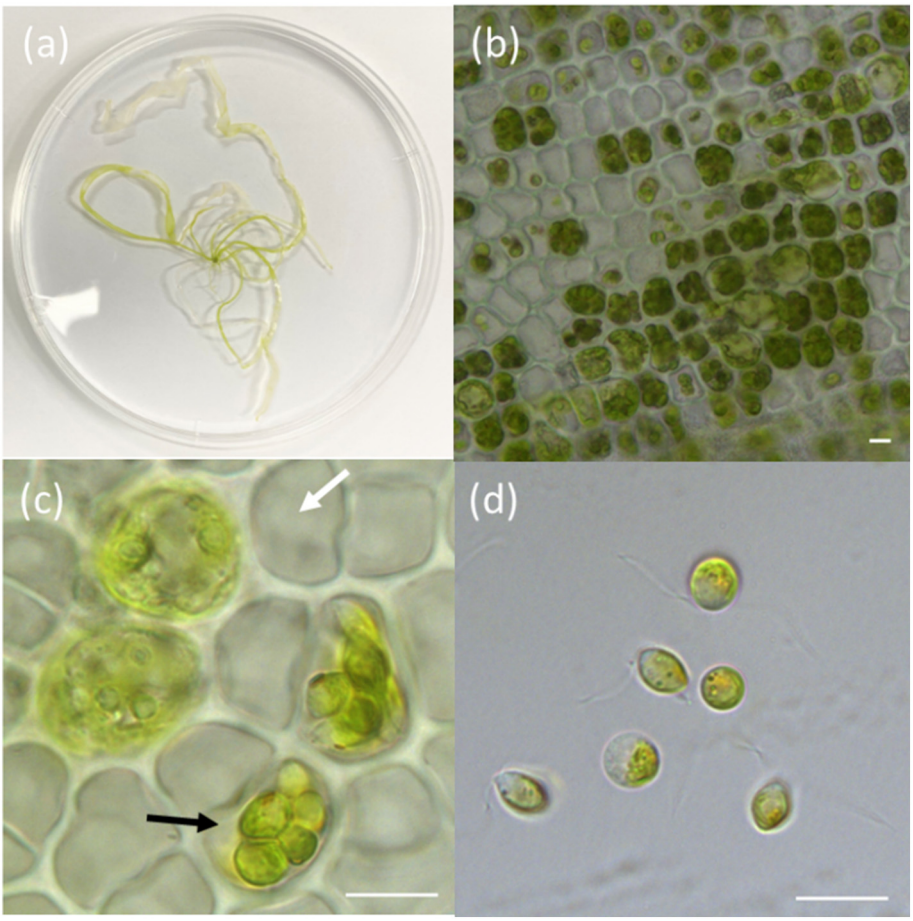

Fig. 1. Light micrographs of *U. intestinalis* in the process of reproduction. (a) Thalli under LNHW$^+$ incubated for 6 days, (b) reproductive cells discharging gametes, (c) sporangia (black arrow; white arrow means empty cells after discharge), and (d) discharged pyriform gametes. The scale bars represent 10 μm.

and Swissprot databases. Gene Ontology (GO) annotation was performed after combining the Blast2GO v2.5.0 results with the NR annotations (Conesa et al., 2005), and DIAMOND v0.8.31 was used to perform Plant Resistance Gene Database (PRGdb) annotation (Buchfink et al., 2014). FDR ≤ 0.001 and the absolute value of $|\log_2 \text{Fold Change}| \geq 1$ were counted as the threshold to judge the significance of gene expression difference between various treatment conditions. GO and KEGG functional enrichment analysis of differentially expressed genes (DEGs) was performed using the phyper function in R software. FDR correction was applied to the *p*-value, with *q*-value ≤ 0.05 were considered significantly enriched.

2.9. Statistical analysis

All data analyses in this study were expressed through replicates ± standard deviation and used the software SPSS v.26. Data under every treatment was confirmed to a normal distribution (Shapiro-Wilk, $P > 0.05$), and the variances were equal (Levene's test, $P > 0.05$). The data for reproduction rate under LNHW$^+$ after day 10 did not abide by a normal distribution because all samples reached a 100% of sporulation. In this case, ANOVA, including repeated measures ANOVA, can still be used because we have a balanced design (Keselman et al., 1996). Repeated measures ANOVA was conducted to assess the effects of culture time on biomass, *Fv/Fm*, Chl *a*, Chl *b*, carotenoids, PE, reproduction rate and C/N content because the same thalli were used for the measurements at different time points (Gao et al., 2018c). Two-way ANOVA was conducted to assess the effects of nitrate and heatwaves on the parameters above. Least significant difference (LSD) was conducted for post hoc investigation. A confidence interval of 95% was set for all tests.

3. Results

3.1. Changes of biomass over time

Changes in biomass of *U. intestinalis* (Fig. 2a) and *G. lemaneiformis* (Fig. 2b) under different nitrate and heatwaves conditions were recorded. The biomass of *U. intestinalis* varied significantly with incubation time under different conditions during 24 days of culture (Table S1) and there was an interactive effect of culture time and nitrate (Table S1). During the temperature-rising period, the biomass of *U. intestinalis* under LN kept increasing while that under HN maintained stable. Across the temperature-maintaining period, the biomass under LNHW$^+$ reached the peak on day 10, while biomass under other treatments continued to increase. During temperature-decreasing period, biomass at LNHW$^-$ began to decrease on day 16 while biomass at HN continued to increase until the end of recovery period. For each time point, nitrate or heatwaves did not significantly affect biomass except for day 12 where nitrate had a significant effect (Table S2).

Regarding *G. lemaneiformis* biomass, culture time had an interactive effect with, nitrate (Table S1) or heatwaves (Table S1). Biomass of *G. lemaneiformis* continued to increase during temperature-rising period, and there was no significant difference among treatments. However, during temperature-maintaining period, the biomass under LNHW$^+$ and HNHW$^+$ both declined after reaching the peaks on day 6, and thalli gradually bleached and completely died by the end of this phase while biomass under HW$^-$ did not show a significant decreasing trend. Although the biomass under HNHW$^-$ appeared to decrease on day 12 compared to that under LNHW$^-$, the difference was not statistically significant (Table S3),

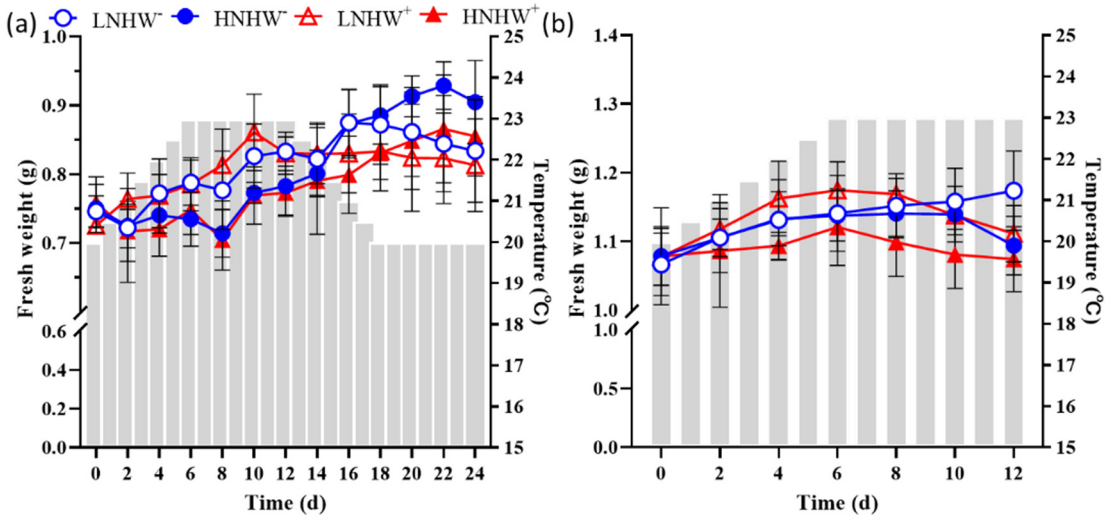

Fig. 2. Biomass changes of *U. intestinalis* (a) and *G. lemaneiformis* (b) grown under various nitrate levels (8 μmol L^{-1}, LN; 200 μmol L^{-1}, HN) and heatwaves conditions during culture periods. Grey bars represent incubation temperature.

thalli under $HNHW^{-}$ being not bleaching either. The experiment was thus ended due to the death of *G. lemaneiformis* under two heatwaves treatments.

3.2. Photosynthesis comparisons between two macroalgae

The maximal photochemical efficiency of PSII (*Fv/Fm*) of two macroalgae under various conditions was also measured (Fig. 3). There were interactive effects of culture time with nitrate (Table S1) and culture time with nitrate and heatwaves on *Fv/Fm* of *U. intestinalis* during 24 days of culture (Table S1). The *Fv/Fm* of *U. intestinalis* under each treatment decreased with culture time, with $LNHW^{+}$ leading to the highest decreasing rate, followed by $LNHW^{-}$ and $HNHW^{-}$, and $HNHW^{+}$ resulting in the lowest decreasing rate. On days 6, 12, and 18, heatwaves did not affect *Fv/Fm* of *U. intestinalis* while HN increased it by 5.91–23.32% (Table S2 and Fig. 3a). On day 24, nitrate and heatwaves showed an interactive effect; heatwaves reduced *Fv/Fm* under LN, but did not significantly affect it under HN (Table S2 and Fig. 3a). In terms of *G. lemaneiformis* (Fig. 3b), culture time and heatwaves had an interactive effect, with *Fv/Fm* under heatwaves having a larger decrease with time (Table S1). Based on two-way ANOVA (Table S3), an interactive effect of nitrate and heatwaves and a main effect of heatwaves were found on day 6; heatwaves reduced *Fv/Fm* by 45.74% under LN while 27.54% at HN. On day 12, heatwaves reduced *Fv/Fm* by 66.95% and 35.87% under LN and HN, respectively.

3.3. Photosynthetic pigments content

The changes of photosynthetic pigments in *U. intestinalis* and *G. lemaneiformis* grown under varying nitrate and heatwaves conditions were showed in Fig. 4. There were interactive effects of culture time with nitrate on Chl *a* (Table S1) and Chl *b* (Table S1) of *U. intestinalis* during 24 days of culture. The Chl *a* and Chl *b* of *U. intestinalis* under LN decreased with culture time, while those under HN exhibited a steep increase on day 6 then decreased with culture time. Carotenoids content also varied with culture time (Table S1), with an increase on day 6 and then decreasing. Nitrate was the main factor influencing pigments content of *U. intestinalis* during the whole culture period. From days 6 to 24, HN increased the contents of Chl *a* (35.92–67.07%), Chl *b* (31.78–62.92%) and carotenoids (39.03–59.21%) in *U. intestinalis* (Table S2 and Fig. 4a–c),

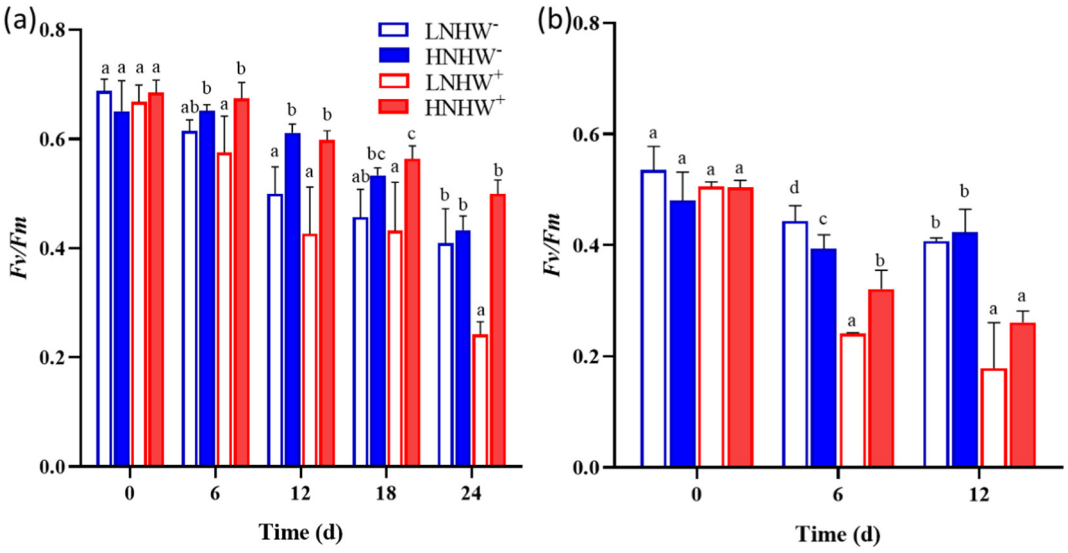

Fig. 3. Maximal photochemical efficiency of PSII (*Fv/Fm*) of *U. intestinalis* (a) and *G. lemaneiformis* (b) grown under various nitrate levels (8 μmol L^{-1}, LN; 200 μmol L^{-1}, HN) and heatwaves conditions. Different letters above bars represent significant differences among treatments ($P < 0.05$).

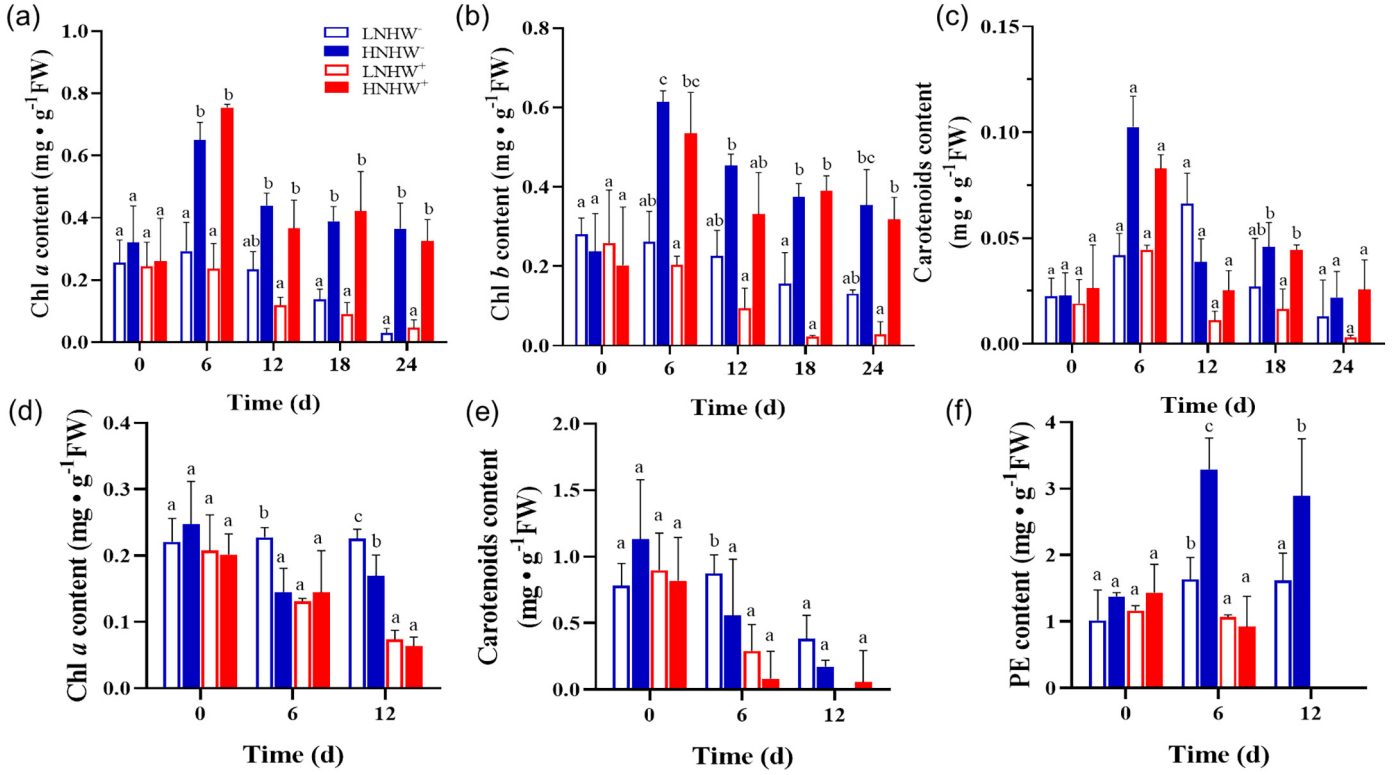

Fig. 4. Pigments contents of *U. intestinalis* (a, b, c) and *G. lemaneiformis* (d, e, f) grown under various nitrate levels (8 μmol L^{-1}, LN; 200 μmol L^{-1}, HN) and heatwaves conditions. Carotenoids under $LNHW^{+}$ and PE under HW^{+} on day 12 were undetectable for *G. lemaneiformis*. Different letters above bars represent significant differences among treatments ($P < 0.05$).

forming greener thalli compared to LN (Fig. 5a), while these pigments were not affected by heatwaves. In contrast, culture time interacted with heatwaves on Chl *a* (Table S1), carotenoids (Table S1) and PE (Table S1) of *G. lemaneiformis* during 12 days of culture. The contents of Chl *a*, carotenoids and PE under heatwaves treatments decreased significantly with culture time, while those without experiencing heatwaves showed no (Chl *a* and PE) or a slight decrease (carotenoids). Heatwaves were the principal factor that reduced the content of Chl *a* (42.40%), carotenoids (66.77–85.03%), and PE (34.93–72.10%) respectively on days 6, resulting in the bleaching of *G. lemaneiformis* (Fig. 5b). On day 12, the carotenoids content under $LNHW^{+}$ and PE content under HW^{+} were even undetectable.

3.4. Reproduction rate

The reproduction rate of *U. intestinalis* varied significantly with incubation time (Table S1); there were interactive effects of culture time and nitrate (Table S1), and culture time, nitrate and heatwaves (Table S1), indicating the change patterns were inconsistent among different conditions. By day 4, thalli under each condition showed reproduction feature

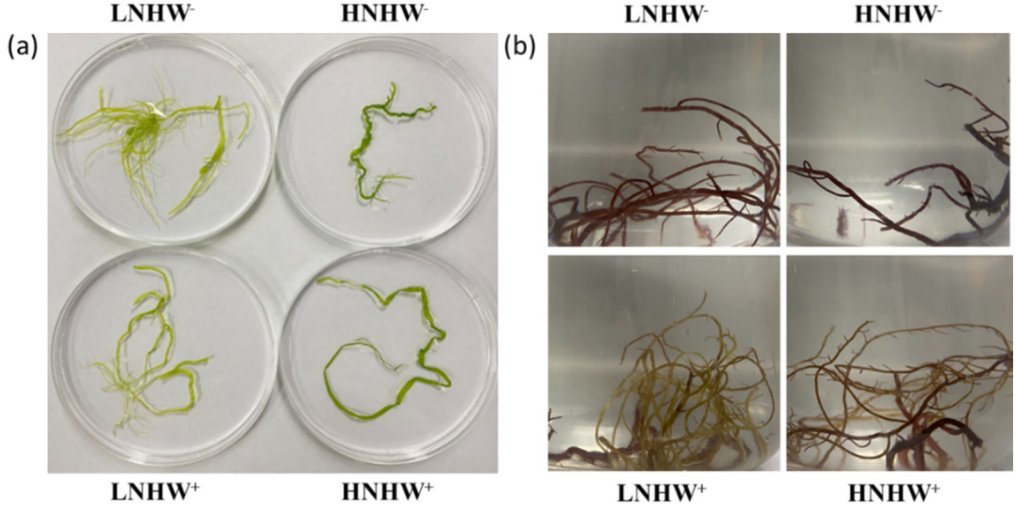

Fig. 5. Color and morphological changes of *U. intestinalis* (a) and *G. lemaneiformis* (b) grown under various nitrate levels (8 μmol L^{-1}, LN; 200 μmol L^{-1}, HN) and heatwaves conditions on day 12.

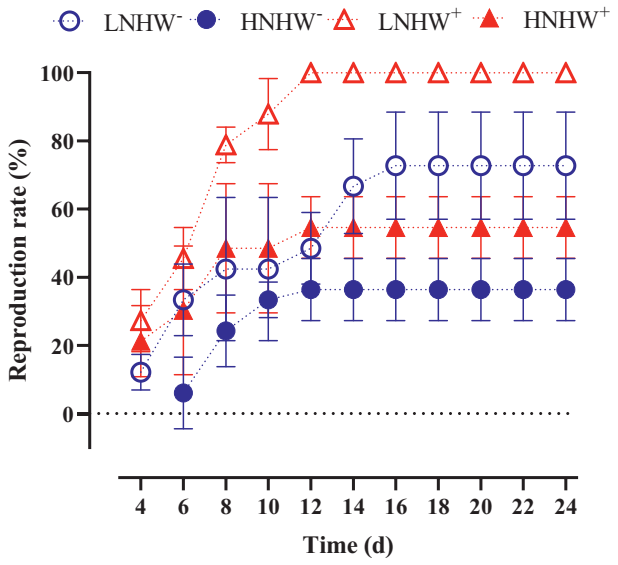

Fig. 6. Reproduction rate of *U. intestinalis* grown under various nitrate levels (8 μmol L^{-1}, LN; 200 μmol L^{-1}, HN) and heatwaves conditions.

except for that under $HNHW^-$ (Fig. 6). By day 6, reproduction events of thalli under $HNHW^-$ occurred. On days 6, 8 and 10, HN reduced while heatwaves stimulated reproduction rate (Table S4). By day 12, thalli under all conditions achieved maximum reproduction rates except for $LNHW^-$. Thalli under $LNHW^+$ had the highest maximum reproduction rate (100 ± 0%), followed by $HNHW^+$ (55 ± 7%) and $LNHW^-$ (48 ± 9%). By day 16, thalli under $LNHW^-$ reached the maximum reproduction rate (73 ± 13%). These results indicate that heatwaves shortened reproduction period and promoted the maximum reproduction rate, while HN alleviated the effects of the heatwaves on reproduction rate. In terms of *G. lemaneiformis*, there were no reproduction events occurring during the experiment.

3.5. Summary of DEGs under various conditions

Differential expression genes (DEGs) were identified using the criteria of ±2 fold change (FC) in expression with q-value < 0.05 between treatments. Although the treatments of nitrate and heatwaves resulted in DEGs for both *U. intestinalis* and *G. lemaneiformis*, the distribution of the DEGs differed between two macroalgae (Fig. 7a–d). For *U. intestinalis*, the differential expression (DE) analysis using t-tests and q-value < 0.05 revealed 59,377 DEGs between $LNHW^-$ and $HNHW^+$, 893 DEGs between $LNHW^-$ and $LNHW^+$, and 12,910 DEGs between $LNHW^-$ and $HNHW^-$ on day 7 (temperature-maintaining period). At the end of the experiment (day 24), there were 22,892 DEGs between $LNHW^-$ and $HNHW^+$, with only 609 DEGs between $LNHW^-$ and $LNHW^+$, and 6,235 DEGs between $LNHW^-$ and $HNHW^-$ (Fig. 7a). Therefore, nitrate had a stronger effect on *U. intestinalis* than heatwaves in terms of the number of DEGs, and the combination of the heatwaves and nitrate resulted in more changes compared to nitrate or heatwaves alone. Meanwhile, the transcriptional response became weaker after the recovery period (Fig. 7b).

In terms of *G. lemaneiformis*, gene transcription only at the beginning of temperature-maintaining period was measured because thalli under heatwaves died by the end of this phase due to bleaching. On day 6, the DE analysis revealed 161 DEGs between $LNHW^-$ and $LNHW^+$, 62 DEGs between $LNHW^-$ and $HNHW^-$, and 123 DEGs between $LNHW^-$ and

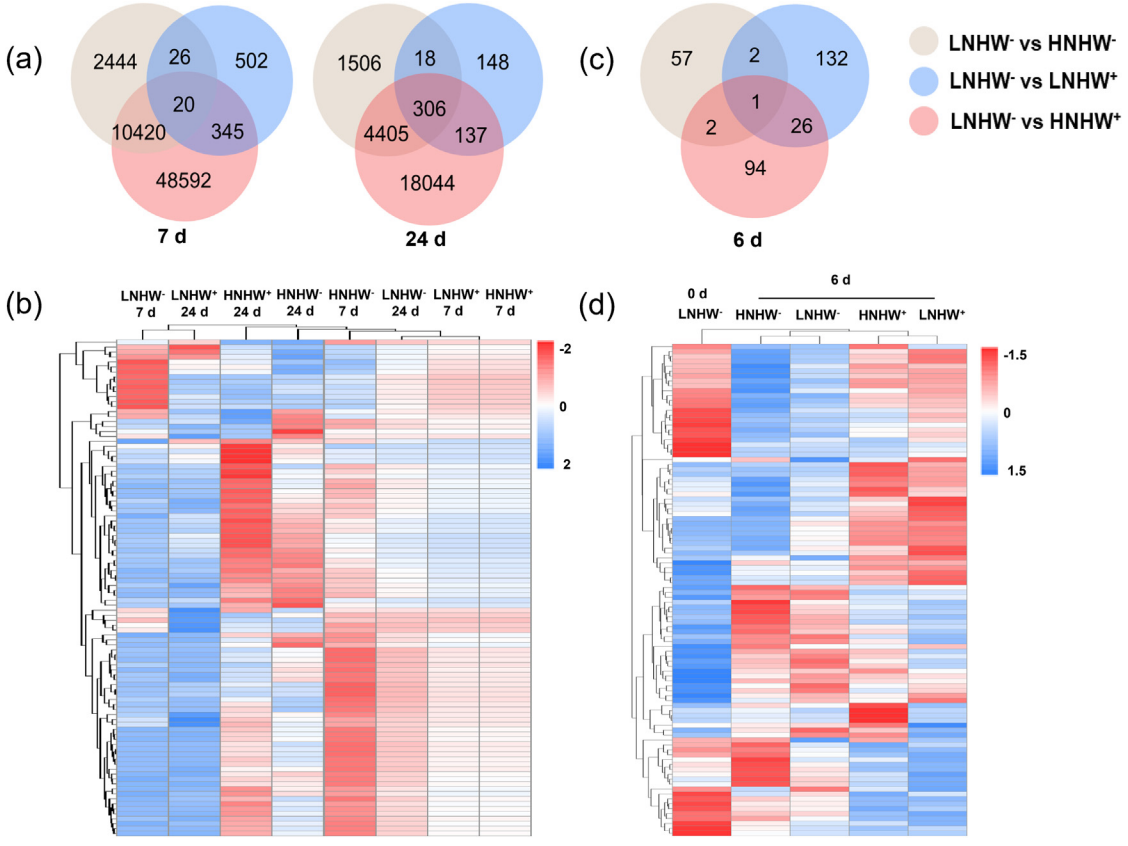

Fig. 7. Differentially expressed genes (DEGs) in *U. intestinalis* and *G. lemaneiformis* subjected to different treatments. (a) Venn diagram of the number of shared or unique *U. intestinalis* DEGs under $LNHW^-$ vs $HNHW^-$, $LNHW^-$ vs $LNHW^+$ and $LNHW^-$ vs $HNHW^+$ on days 7 and 24. (b) Heatmap of the relative expression of *U. intestinalis* genes under various treatments on days 7 and 24. (c) Venn diagram of the number of shared or unique *G. lemaneiformis* DEGs under $LNHW^-$ vs $HNHW^-$, $LNHW^-$ vs $LNHW^+$ and $LNHW^-$ vs $HNHW^+$ on day 6. (d) Heatmap of the relative expression of *G. lemaneiformis* genes following under various treatments on day 6.

HNHW$^+$ (Fig. 7c). The heatwaves thus led to larger transcriptional response compared to nitrate. The same pattern could be seen in the heatmap, where LNHW$^-$ and HNHW$^-$ gathered, with LNHW$^+$ and HNHW$^+$ being in the same cluster (Fig. 7d).

3.6. Transcriptomic response of *U. intestinalis* to nitrate enrichment and heatwaves

To clearly demonstrate how nitrate affected the transcriptome of *U. intestinalis*, the two groups (LNHW$^-$ vs HNHW$^-$) were singled out for comparison. Compared to the LNHW$^-$ group, the HNHW$^-$ group had 4050 (1.38%) upregulated and 753 (0.26%) downregulated genes on day 7, and 2399 (0.27%) upregulated and 784 (0.81%) downregulated genes on day 24 (Fig. 8a). To assess the biological significance of DEGs by KEGG pathway enrichment analysis, a summary of pathways with significant enrichment of DEGs between the LNHW$^-$ and HNHW$^-$ groups was screened at q-value < 0.05 (Fig. 8b). The pathway enrichment analysis showed that the photosynthesis-antenna proteins and photosynthesis were the most significantly enriched pathways both on days 7 and 24 in the DEGs (Fig. 8b). In photosynthesis, genes related to photosystem I (*PsaB*, *PsaE*, *PsaF*, *PsaG*, *PsaH*, *PsaL*, *PsaO*), light-harvesting chlorophyll protein (*Lhca1*, *Lhca3*, *Lhca5*, *Lhcb1*, *Lhcb2*, *Lhcb4*) and photosynthetic electron transport (*PetE*, *PetF*) were significantly upregulated 2.8–6.8 $\log_2$ folds on day 7 and 1.7–6.3 $\log_2$ folds on day 24 by nitrate enrichment, respectively (Fig. 8c). Another notable pathway is nitrogen and glutathione metabolism. Genes involved in nitrogen transport pathway, such as *Nrt*, *NR* and *glnA* were significantly downregulated 2.1–8.7 $\log_2$ folds on day 7, and genes related to the glutathione metabolism pathway (*gdhA*, *GLT1*, *gshA*, *GSR*, *TXNDC12*, *gpx*, *DHAR*, *G6PD*, *ODC1*, *argJ*, *argE*, *argD*) were significantly upregulated 2.7–9.7 $\log_2$ folds on day 24 (Fig. 8d).

Two groups (LNHW$^-$ vs LNHW$^+$) respectively on days 7 and 24 were compared to figure out the influence of heatwaves on transcriptomes of *U. intestinalis* (Fig. 9a–d). Compared to the LNHW$^-$ group, 603 (0.21%) upregulated and 52 (0.02%) downregulated genes were identified on day 7, and 126 (0.04%) upregulated and 60 (0.02%) downregulated genes were identified on day 24 for the LNHW$^+$ group (Fig. 9a). The number of DEGs caused by heatwaves was less than that of DEGs caused by nitrate enrichment, suggesting that nitrate had a stronger impact on *U. intestinalis*. For KEGG enrichment pathway analysis, the citrate cycle (TCA cycle) and oxidative phosphorylation were remarkable pathways affected by heatwaves (Fig. 9b). Genes related to oxidative phosphorylation, such as NADH dehydrogenase (*Ndufs4*, *Ndufs7*, *Ndufs8*, *Ndufv1*, *Ndufv2*, *Ndufab1*, *Ndufab12*, *Ndufab9*), succinate dehydrogenase/fumarate reductase (*SDHC*, *SDHD*, *SDHA*, *SDHB*), cytochrome c reductase (*ISP*, *Cyt 1*, *QCR6*, *QCR7*), cytochrome c oxidase (*COX6A*, *cox6B*) and F-type ATPase (*beta*, *gamma*, *delta*, *epsilon*, *OSCP*), were significantly upregulated 2.4–5.2 $\log_2$ folds on day 7 (Fig. 9c). Meanwhile, genes involved in TCA cycle such as *CS*, *ACO*, *IDh1*, *OGDH* were significantly upregulated 3.4–5.4 $\log_2$ folds on day 7 (Fig. 9d).

Comparisons between two groups (LNHW$^-$ vs HNHW$^+$) respectively on days 7 and 24 were conducted to investigate the combined effects of nitrate and heatwaves (Fig. 10a–d). Compared to the LNHW$^-$ group, 20,619 (6.68%) upregulated and 9449 (3.06%) downregulated genes were identified in the HNHW$^+$ group on day 7, and 10,854 (3.46%) upregulated and 2383 (0.76%) downregulated genes were identified on day 24 (Fig. 10a). The outcome of KEGG pathway enrichment analysis was similar to nitrate enrichment alone, which displayed that the photosynthesis-antenna proteins and photosynthesis were the most significantly enriched pathways both on days 7 and 24 (Fig. 10b). Genes related to photosynthesis were significantly upregulated 2.3–7.8 $\log_2$ folds on day 7 and 2.5–9.8 $\log_2$ folds on day 24, respectively (Fig. 10c). In the meantime, genes involved in nitrogen transport pathway, such as *Nrt* and *NR,* were significantly downregulated 6.8–9.9 $\log_2$ folds on day 7, and genes related to the glutathione metabolism pathway (*nirA*, *gdhA*, *glnA*, *GLU*, *GSR*, *gpx*, *DHAR*, *ODC1*, arg*J*, *argE*, *argD*, *argB*, *argC*, *argF*, *arg*, *speE*, *IDH1*) were significantly upregulated 4.7–8.8 $\log_2$ fold on day 24 (Fig. 10d). The proportion and fold change of DEGs were significantly increased under the combination of nitrate enrichment and heatwaves compared to nitrate or heatwaves alone. Compared to nitrogen enrichment alone, genes related to photosystem II (*PsaB*, *PsaD*, *PsaE*, *PsaF*, *PsaH*, *PsaL*, *PsaO*) were significantly upregulated and urea cycle-related genes (*argG*, *argH*, *argF*, *arg*) were altered.

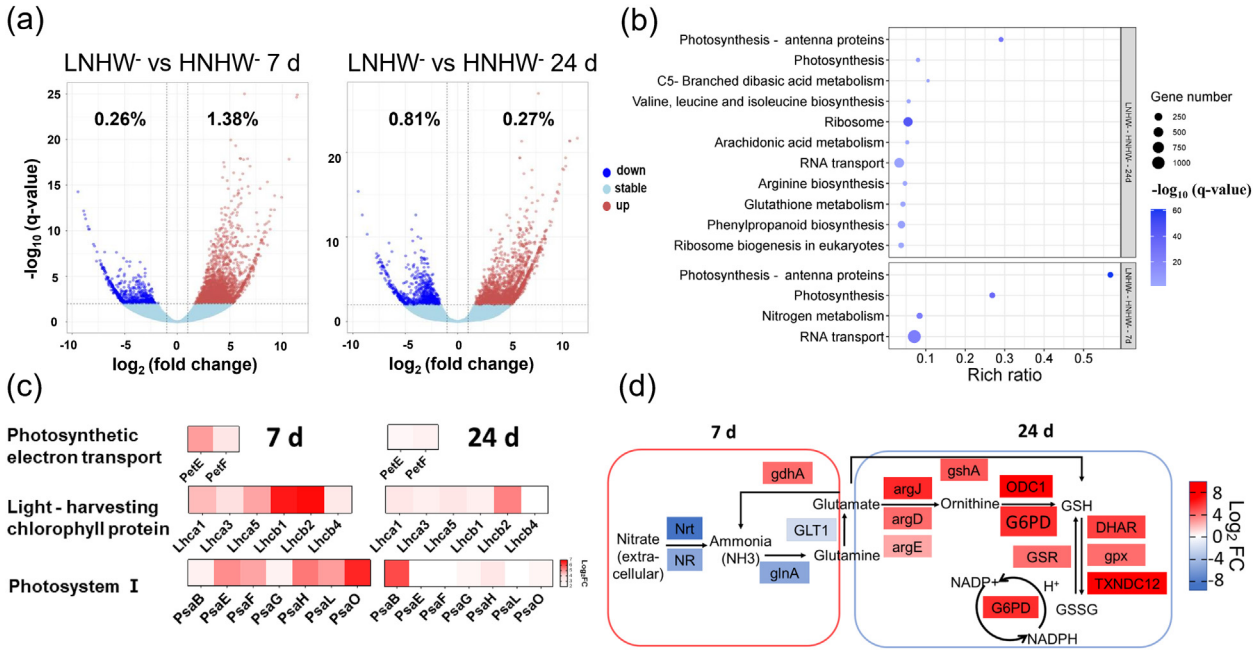

Fig. 8. Differentially expressed genes (DEGs) between LNHW$^-$ and HNHW$^-$ groups and related pathway for *U. intestinalis*. (a) Comparison of expression patterns of DEGs identified between LNHW$^-$ and HNHW$^-$ groups on days 7 and 24. The red (right) and blue (left) dots represent up or downregulated DEGs respectively, and the grey dots represent non-DEGs. (b) KEGG pathway enrichment analysis of DEGs. The vertical axis represents the pathway name and the horizontal axis is rich ratio. The figure only shows the pathway whose q-value < 0.05. (c) Heatmap of genes related to photosynthesis. The color represents the difference in $\log_2$ fold. (d) Changes in expression of genes associated with the nitrogen and glutathione pathways. The red and blue color represents upregulation and downregulation, respectively.

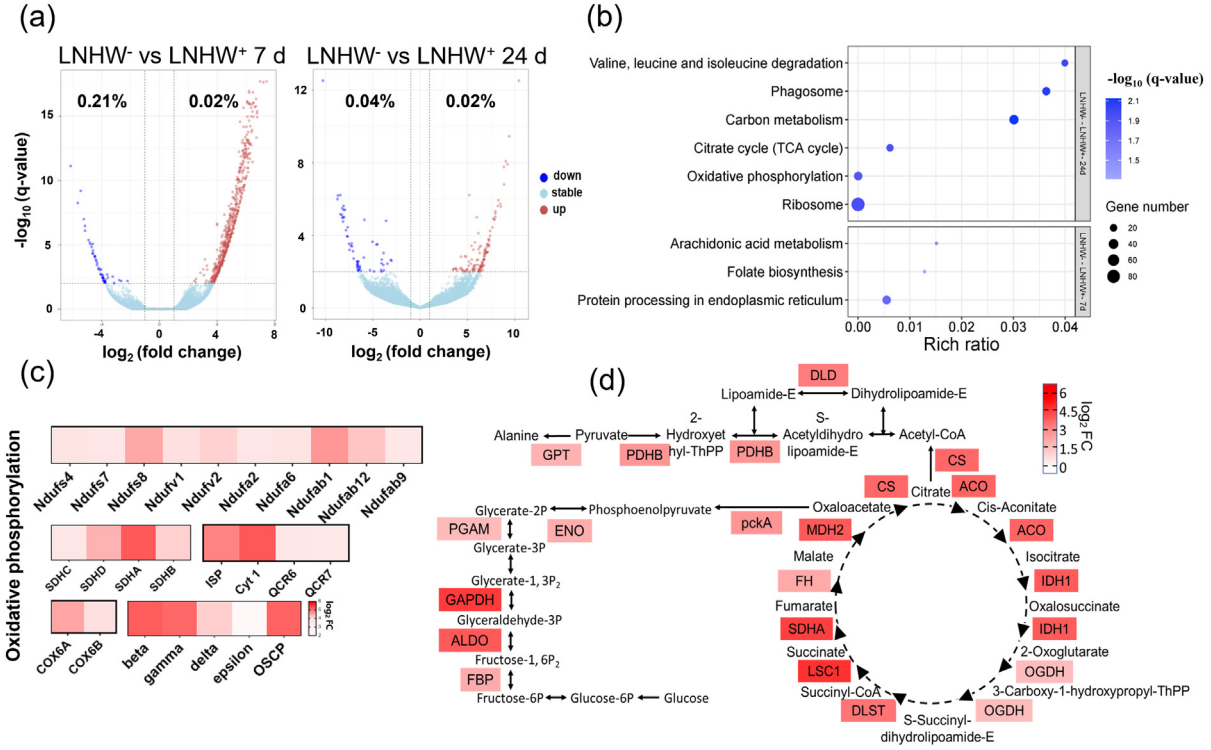

Fig. 9. Differentially expressed genes (DEGs) between LNHW$^-$ and LNHW$^+$ groups and related pathway for *U. intestinalis*. (a) Comparison of expression patterns of DEGs identified between LNHW$^-$ and LNHW$^+$ groups on days 7 and 24 for *U. intestinalis*. The red (right) and blue (left) dots represent up or downregulated DEGs, and the grey dots represent non-DEGs. (b) KEGG pathway enrichment analysis of DEGs. The vertical axis represents the pathway name and the horizontal axis is rich ratio. The figure only shows the pathway whose q-value < 0.05. (c) Heatmap of genes related to oxidative phosphorylation on day 7. The color represents the difference in $\log_2$ fold. (d) Changes in expression of genes associated with the citrate cycle pathways on day 7.

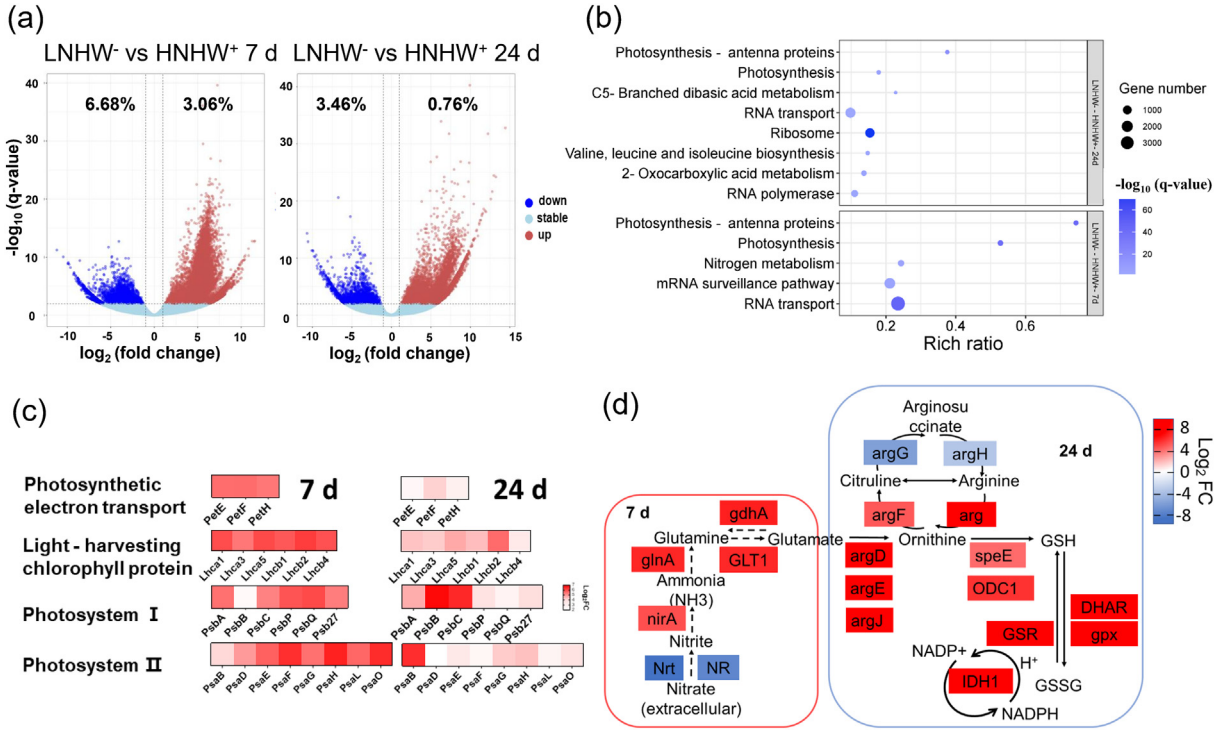

Fig. 10. Differentially expressed genes (DEGs) between LNHW$^-$ and HNHW$^+$ groups and related pathway for *U. intestinalis*. (a) Comparison of expression patterns of DEGs identified between LNHW$^-$ and HNHW$^+$ groups on days 7 and 24. The red (right) and blue (left) dots represent up or downregulated DEGs, and the grey dots represent non-DEGs. (b) KEGG pathway enrichment analysis of DEGs. The vertical axis represents the pathway name and the horizontal axis is rich ratio. The figure only shows the pathway whose q-value < 0.05. (c) Heatmap of genes related to photosynthesis. The color represents the difference in $\log_2$ fold. (d) Changes in expression of genes associated with the nitrogen and glutathione pathways.

3.7. Transcriptomic response of G. lemaneiformis to nitrate enrichment and heatwaves

Changes on transcripts of *G. lemaneiformis* under different treatments were also analyzed to figure out the effect of each factor (Fig. 11a–f). However, the number of genes in *G. lemaneiformis* was much fewer than that of *U. intestinalis*, which resulted in less information. Groups on day 6 were compared to demonstrate the effects of nitrate ($LNHW^-$ vs $HNHW^-$), heatwaves ($LNHW^-$ vs $LNHW^+$) and their interactions ($LNHW^-$ vs $HNHW^+$). On day 6, 46 (0.06%) upregulated and 18 (0.l5%) downregulated genes were identified in the $HNHW^-$ group compared to the $LNHW^-$ group (Fig. 11a), 77 (0.44%) upregulated and 86 (0.4%) downregulated genes were identified in the $LNHW^+$ group compared to the $LNHW^-$ group (Fig. 11b), and 81 (0.17%) upregulated and 44 (0.32%) downregulated genes were identified in the $HNHW^+$ group compared to the $LNHW^-$ group (Fig. 11c). The most distinctly changed pathway was photosynthesis. The outcome of KEGG pathway enrichment analysis of nitrate enrichment alone displayed that secondary metabolite biosynthesis like stibenoid, diarytanoid, gingerol and flavonoid were significantly impacted (Fig. 11d). Genes related to photosystem II (*PsbO*, *PsbQ*, *PsbU*) were significantly downregulated 1.7–2.4 $\log_2$ folds under heatwaves treatment on day 6 (Fig. 11e), but upregulated 4.9–5.6 $\log_2$ folds under heatwaves + nitrate treatment. Meanwhile, genes related to light-harvesting chlorophyll protein (*Lhca1*, *Lhca3*, *Lhca5*, *Lhcb1*, *Lhcb2*, *Lhcb4*, *Lhcb5*) were upregulated 4.7–7.6 $\log_2$ folds under heatwaves + nitrate treatment on day 6 (Fig. 11f).

4. Discussion

4.1. Response of U. intestinalis to heatwaves regulated by nitrate availability

Nitrogen enrichment can usually increase biomass and growth of macroalgae, including *Ulva* spp. (Tyler et al., 2005; Gao et al., 2018a; Traugott et al., 2020). However, different result was found in this study. *U. intestinalis* cultured with LN showed continuous growth during first 8 days, forming numerous and slender algal branches, while the algae cultured with HN possessed stable biomass and fewer and shorter algal branches. One possible reason for this is the change of culture conditions. The algae were cultured for one week using the natural seawater before conducting the experiment. After experiencing this nitrogen-deficient period (0–8 μmol L^{-1}), the thalli prefer to synthesize the photosynthetic proteins and pigments and reserve nutrients rather than grow when nutrients are added (Kumari et al., 2014; Chen et al., 2019). Meanwhile, thalli cultured under LN treatment could utilize stored nutrients to form more branches for expanding the surface area in contact with seawater to absorb more nutrients, which contributed to increased biomass (Ma et al., 2020). However, this pattern varied with culture period. Thalli cultured with HN began to grow after restoring while the biomass of thalli cultured with LN

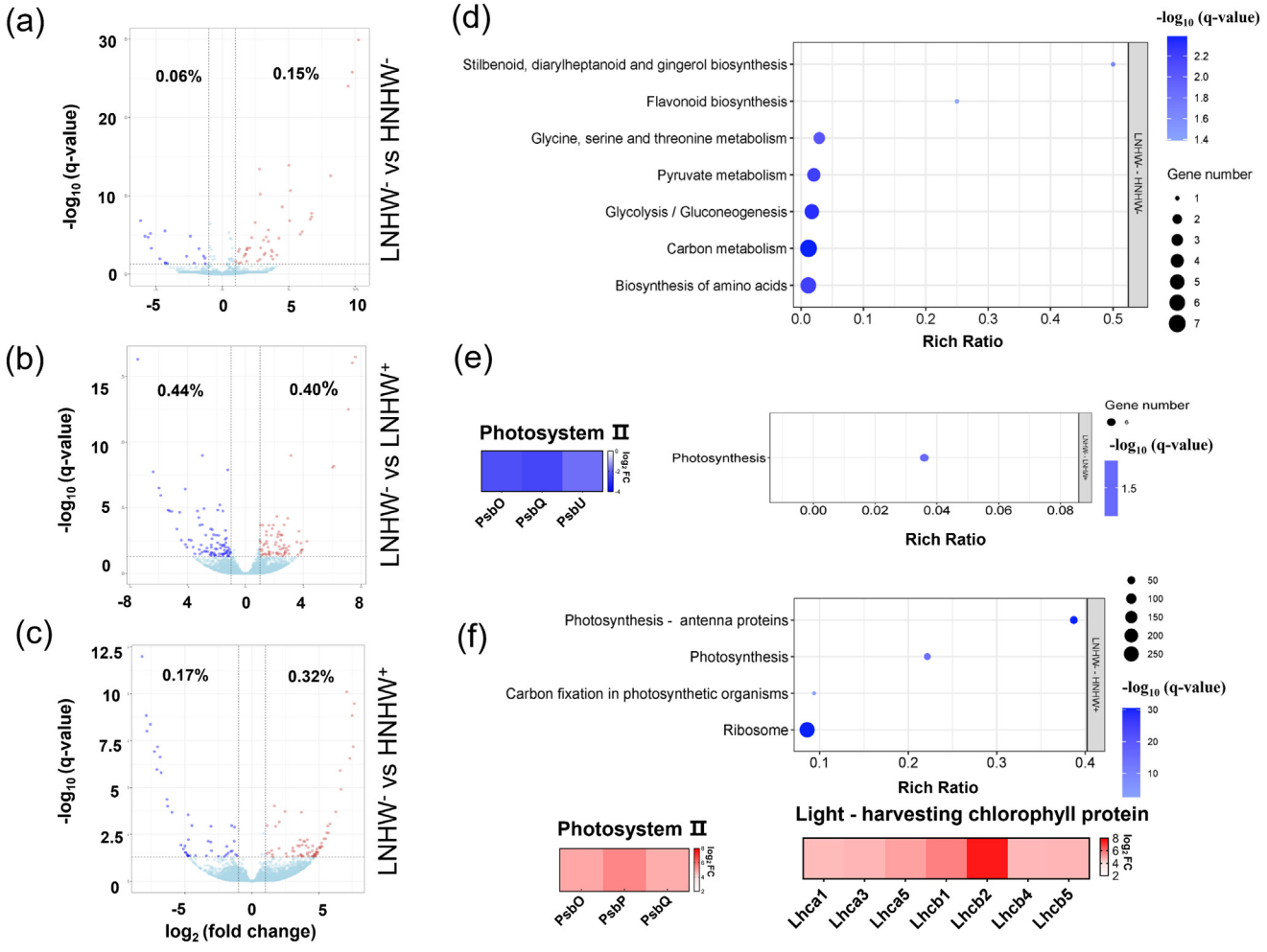

Fig. 11. Differentially expressed genes (DEGs) between different groups for *G. lemaneiformis*. (a), (b), (c) Expression patterns of DEGs identified between $LNHW^-$ and $HNHW^-$, $LNHW^-$ and $LNHW^+$, $LNHW^-$ and $HNHW^+$ groups, respectively, on day 6. The red (right) and blue (left) dots represent up or downregulated DEGs, and the grey dots represent non-DEGs. (d), (e), (f) KEGG pathway enrichment analysis of DEGs and heatmap of genes related to photosynthesis for $LNHW^-$ vs $HNHW^-$, $LNHW^-$ vs $LNHW^+$, $LNHW^-$ vs $HNHW^+$, respectively. The vertical axis represents the pathway name and the horizontal axis is rich ratio. The figure only shows the pathway whose q-value < 0.05. The color represents the difference in $\log_2$ fold.

declined when nitrogen could not be supplied for a long time. In this study, the *Fv/Fm* and photosynthetic pigments of *U. intestinalis* under HN treatment increased, which is consistent with other findings in *Ulva* species (Gordillo et al., 2001; Figueroa-Torres et al., 2017). Genes related to nitrogen-transport (*Nrt*, *NR*) were significantly down-regulated and genes related to photosynthesis were significantly up-regulated on day 7, suggesting that *Ulva* no longer needed synthesizing abundant nitrogen-transport proteins to take up nitrogen from the environment, but rather to enhance photosynthesis in preparation for increased biomass. The biomass of $LNHW^-$ treatment declined after reaching a maximum at day 16 while that of $HNHW^-$ treatment declined from day 22, which supports the important role of nitrogen in the growth of *U. intestinalis*. During the growth of plant, free radicals are constantly produced by the metabolism of the organism, which leads to ageing and death (Yang and Gao, 2001). In this study, the expression of key enzymes in the glutathione metabolic pathway of *U. intestinalis* under HN environment was significantly changed. Glutathione reductase (GSR) catalyzes the reduction of glutathione disulphide (GSSG) to the sulphydryl form glutathione (GSH), which is a crucial molecule in resisting oxidative stress and maintaining the intracellular reducing environment (Vanacker, 2000; Deponte, 2013). This suggests that in an environment with sufficient nitrogen, *U. intestinalis* could synthesize increased GSH to scavenge its free radical production, thereby enhancing its capacity to address environmental stress. At the end of the experiment, the tissue nitrogen content was also significantly higher under HN than LN (Fig. S3). The nitrogen content of *U. intestinalis* in this study falls in the range of *Ulva* species reported in previous studies (Table S5).

It has been demonstrated that the MHWs usually reduce macroalgae biomass by negatively affecting photosynthesis (Rendina et al., 2019). In the present study, MHWs also led to an earlier biomass decrease in *U. intestinalis*. However, this decline was not due to the inhibition of photosynthesis since MHWs did not reduce *Fv/Fm* or photosynthetic pigments significantly and genes related to photosynthesis had no prominent change either throughout the experiment. MHWs induced a higher reproduction rate, which could be the critical reason that led to decreased biomass. This phenomenon is supported by the result of transcripts. Genes related oxidative phosphorylation and TCA cycle-related genes were significantly up-regulated, which are closely related to spore formation in *Ulva* species (Wang et al., 2016; Park, 2020). Higher temperatures can usually induce reproduction events of *Ulva* species. For instance, *U. rigida* cultured at 18 °C show noticeable reproduction events while it did not occur in thalli at 14 °C during 12 days of experiment (Gao et al., 2017a). The transformation from vegetative cells to reproductive cells and then the formation of micropropagules is a survival strategy for macroalgae to deal with environmental stress (Gao et al., 2017b; Huo et al., 2021). Our results indicate that *Ulva* species could respond to and survive MHWs through the shift of life history stage.

However, when *U. intestinalis* was cultured in the nitrate-replete condition, it could fully absorb nitrate for the synthesis of photosynthetic proteins and GSH that was able to scavenge free radicals produced by MHWs. Meanwhile, the oxidative phosphorylation and TCA cycle pathways were insignificantly changed, indicating that the thalli may reduce the harm caused by heatwaves by scavenging intracellular free radicals and thus the need of converting vegetative cells into spores to counteract the heatwaves decreased. This explains why thalli cultured at $HNHW^+$ had a lower reproduction rate compared to that at $LNHW^+$. As a local driver, nitrogen can modulate responses of macroalgae to high seawater temperatures, ameliorating their negative impacts on physiological performance such as growth and photosynthesis (Gao et al., 2017a; Fernández et al., 2020). However, the potential molecular mechanisms of nitrogen regulation on MHWs remain unclear. Our study showed that genes related to glutathione metabolism were significantly upregulated, and it is thus possible that the elevated GSH caused by nitrogen metabolism is responsible for the ability of macroalgae to withstand heatwaves under HN conditions. For *U. intestinalis*, nitrogen had a positive effect, while heatwaves had a negative effect, and when the two were coupled, the effect of nitrogen dominated and was able to counteract the negative effect of heatwaves. This pattern was also supported by the Venn diagram; the number of DEGs under nitrogen treatment was much higher than that of under heatwaves.

4.2. Irretrievable death of *G. lemaneiformis* under heatwaves

Nitrate enrichment did not affect the biomass or *Fv/Fm* of *G. lemaneiformis*, which is not entirely consistent with previous studies (Duan et al., 2019; Ma et al., 2021). Nitrogen had a beneficial effect on the growth and capacity for carbon sequestration of *G. lemaneiformis* (Duan et al., 2019), and nitrogen enrichment enhanced the resistance level to high temperature for *G. blodgettii* (Ma et al., 2021). One possible reason is the differences in nitrogen utilization strategies of *G. lemaneiformis* under different nitrogen levels. Compared to day 0, tissue N content of $LNHW^-$ treatment on day 12 had an 80% reduction, while that of $HNHW^-$ exhibited no decrease (Fig. S3). Although biomass of $LNHW^-$ and $HNHW^-$ both continued to increase during culture time, the former could be considered to consume its own stored nitrogen under LN condition, and the latter could utilize nitrogen from environment under HN condition. During the relative short culture period (12 days), the combination of consuming stored nitrogen and absorbing nitrogen from natural seawater (LN) did not fall behind the high nitrogen supply (HN). A similar result was also reported by Zhou et al. (2022). Under the influence of the heatwaves, the biomass of *G. lemaneiformis* cultured at different nitrogen conditions all reached a maximum at the end of temperature-rising period, declined rapidly during temperature-maintaining period and died at the end of temperature-maintaining period, indicating the fatal effect of MHWs on *G. lemaneiformis*. Previous studies show that MHWs could lead to the reduced cover of the dominant kelp in the west coast of Australia (Wernberg et al., 2013) and complete loss (100%) of bull kelp *Durvillaea poha* at Pile Bay in Lyttelton Harbor, the east coast of the South Island of New Zealand (Thomsen et al., 2019). The present study shows that the biomass loss of macroalgae may be caused by the harms of MHWs to photosynthetic apparatus and pigments. Both *Fv/Fm* and photosynthetic pigments of *G. lemaneiformis* were largely reduced when experiencing heatwaves. Furthermore, genes related to photosynthesis were also significantly down-regulated, indicating that the impacts of heatwaves involve both physiological and molecular levels. Another reason that *G. lemaneiformis* could not survive heatwaves can be attributed to the dominance of its vegetative form in its life history. Thalli usually have lower resilience to high temperatures compared to micropropagules (Carney and Edwards, 2006).

In contrast to individual HN treatment, genes related to photosynthesis in *G. lemaneiformis* under the combination of heatwaves and HN were significantly up-regulated, showing that heatwaves urged photosynthetic protein synthesis when nitrogen is sufficient. However, from the Venn diagram, the number of DEGs under heatwaves treatment was much greater than that under nitrogen treatment, indicating that the negative effects of heatwaves may exceed the positive effects of nitrate enrichment. Therefore, the thalli experiencing heatwaves died by day 12. It seems that the shift from thalli to micropropagules for *G. lemaneiformis* is not as easy as *Ulva* (Gao et al., 2010; Zhou et al., 2016) since reproduction events were not found for *G. lemaneiformis* no matter nitrogen was limited or replete, which closed the escape route of *G. lemaneiformis* via life history shift.

4.3. Implications of differential responses of two macroalgae

U. intestinalis could reserve nutrients when the condition is allowed and take advantage of them to maintain stable growth rates when nutrients become limited for a short term. In addition, *U. intestinalis* could counteract nutrient limitation via the change of morphology. When suffering heatwaves stress, *U. intestinalis* could transform vegetative cells into resistant spores. Thus, *U. intestinalis* may be adapting to climate change and related extreme weather by shortening its life cycle. Shorter generation times imply more opportunities to adapt phenotypically and genetically to climate change (Gao et al., 2017b). Meanwhile, when nutrients were replete, *U. intestinalis* could utilize nutrients to counteract heatwaves in the form of thalli and reduce the shift to micropropagules. To summarize, *Ulva* seems to

be able to acclimate to different environmental conditions via morphological, physiological and molecular modulation. The strong resilience to environmental stress would increase the competitiveness of *Ulva* spp. against other seaweeds, which may promote the outbreak of green tides caused by *Ulva* spp. in the future.

On the other hand, the economic algae *G. lemaneiformis*, was prone to bleaching and died under heatwaves. Although nitrogen enrichment supported thalli to counteract the negative effect of the heatwaves, the death of the *G. lemaneiformis* could not be prevented ultimately. As previously mentioned, along with the increasing ocean temperature, a gradual reduction in the competency of either reproduction, recruitment, or recruit survival was found in kelps (Wernberg et al., 2010). Combined with the previous study, the findings in this study indicate that MHWs may exert a negative influence on seaweed cultivation. It has been presumed that MHWs are impacting the structure of macroalgae, facilitating the thriving of morphologically simple, ephemeral and opportunistic turfs (Gao et al., 2021). Our study confirms this presumption and justifies this conclusion regardless of nitrate conditions.

5. Conclusion

MHWs are impacting algal structure and primary production. The present study investigated the combined effects of MHWs and nitrate availability on a bloom-forming green macroalga *U. intestinalis* and an economically important red macroalga *G. lemaneiformis* for the first time. *U. intestinalis* formed more branches under nitrate limited conditions and transformed from thalli to micropropagules to cope with MHWs. When nitrate was replete, thalli upregulated their antioxidant systems to counteract MHWs and downregulated the shift to micropropagules. These findings suggest the diverse and flexible strategies of *U. intestinalis* to respond to changing environments. On the other hand, *G. lemaneiformis* did not survive MHWs even when nitrate was replete. This study indicates that *Ulva* spp. may replace cultivated macroalgae in the future context of climate change considering that they co-occur in seaweed farms. Strains of *G. lemaneiformis* that are tolerant to high temperatures need to be bred to avoid or reduce the loss of seaweed cultivation and inhibit the occurrence of green tides.

CRediT authorship contribution statement

Meijia Jiang: Investigation, Methodology, Formal analysis, Visualization, Writing – original draft, Writing – review & editing. **Lin Gao:** Investigation, Methodology, Writing – review & editing. **Ruiping Huang:** Methodology, Writing – review & editing. **Xin Lin:** Methodology, Writing – review & editing. **Guang Gao:** Conceptualization, Methodology, Formal analysis, Writing – original draft, Writing – review & editing, Supervision, Funding acquisition.

Declaration of competing interest

The authors declare that they have no known competing financial interests or personal relationships that could have appeared to influence the work reported in this paper.

Acknowledgments

This work was supported by the National Natural Science Foundation of China (42076154), the National Key Research and Development Program of China (2018YFD0900703), and the MEL Internal Research Program (MELRI2004).

Appendix A. Supplementary data

Supplementary data to this article can be found online at https://doi.org/10.1016/j.scitotenv.2022.156591.

References

Alan, R., Wellburn, 1994. The spectral determination of chlorophylls *a* and *b*, as well as total carotenoids, using various solvents with spectrophotometers of different resolution. J. Plant Physiol. 144, 307–313.
Beer, S., Eshel, A., 1985. Determining phycoerythrin and phycocyanin concentrations in aqueous crude extracts of red algae. Mar. Freshwater Res. 36 (6), 785–792.
Buchfink, B., Xie, C., Huson, D.H., 2014. Fast and sensitive protein alignment using DIAMOND. Nat. Methods 12, 59–60.
Cabello-Pasini, A., Macías-Carranza, V., Abdala, R., Korbee, N., Figueroa, F.L., 2011. Effect of nitrate concentration and UVR on photosynthesis, respiration, nitrate reductase activity, and phenolic compounds in *Ulva rigida* (Chlorophyta). J. Appl. Phycol. 23, 363–369.
Capo, T.R., Jaramillo, J.C., Boyd, A.E., Lapointe, B.E., Serafy, J.E., 1999. Sustained high yields of *Gracilaria* (Rhodophyta) grown in intensive large-scale culture. J. Appl. Phycol. 11, 143–147.
Carney, L.T., Edwards, M.S., 2006. Cryptic processes in the sea: a review of delayed development in themicroscopic life stages of marine macroalgae. Algae 21, 161–168.
Chen, B., Lin, L., Ma, Z., Zhang, T., Chen, W., Zou, D., 2019. Carbon and nitrogen accumulation and interspecific competition in two algae species, *Pyropia haitanensis* and *Ulva lactuca*, under ocean acidification conditions. Aquac. Int. 27, 721–733.
China Fishery Statistical Yearbook, 2020. 2020. China Agriculture Press, Beijing.
Christie, H., Norderhaug, K.M., Fredriksen, S., 2009. Macrophytes as habitat for fauna. Mar. Ecol. Prog. Ser. 396, 221–233.
Choi, T.S., Kang, E.J., Kim, J.H., Kim, K.Y., 2010. Effect of salinity on growth and nutrient uptake of *Ulva Pertusa* (Chlorophyta) from an eelgrass bed. Algae 25, 17–26.
Conesa, A., Gotz, S., Garcia-Gomez, J.M., Terol, J., Talon, M., Robles, M., 2005. Blast2GO: a universal tool for annotation, visualization and analysis in functional genomics research. Bioinformatics 21, 3674–3676.
Deponte, M., 2013. Glutathione catalysis and the reaction mechanisms of glutathione-dependent enzymes. Biochim. Biophys. Acta-Gen. Subj. 1830, 3217–3266.
Dewey, C.N., Li, B., 2011. RSEM: accurate transcript quantification from RNA-seq data with or without a reference genome. BMC Bioinformatics 12, 323.
Duan, Y., Yang, N., Hu, M., Wei, Z., Bi, H., Huo, Y., He, P., 2019. Growth and nutrient uptake of *Gracilaria lemaneiformis* under different nutrient conditions with implications for ecosystem services: a case study in the laboratory and in an enclosed mariculture area in the East China Sea. Aquat. Bot. 153, 73–80.
Fernández, P.A., Gaitán-Espitia, J.D., Leal, P.P., Schmid, M., Revill, A.T., Hurd, C.L., 2020. Nitrogen sufficiency enhances thermal tolerance in habitat-forming kelp: implications for acclimation under thermal stress. Sci. Rep. 10, 262–269.
Feng, Y., Bethel, B.J., Dong, C., Zhao, H., Yao, Y., Yu, Y., 2022. Marine heatwave events near Weizhou Island, beibu gulf in 2020 and their possible relations to coral bleaching. Sci. Total Environ. 823, 153414.
Feng, Z., Zhang, T., Shi, H., Gao, K., Huang, W., Xu, J., Wang, J., Wang, R., Li, J., Gao, G., 2020. Microplastics in bloom-forming macroalgae: distribution, characteristics and impacts. J. Hazard. Mater. 397, 122752.
Figueroa-Torres, G.M., Pittman, J.K., Theodoropoulos, C., 2017. Kinetic modelling of starch and lipid formation during mixotrophic, nutrient-limited microalgal growth. Bioresour. Technol. 241, 868–878.
Frölicher, T.L., Fischer, E.M., Gruber, N., 2018. Marine heatwaves under global warming. Nature 560, 360–364.
Gao, G., Beardall, J., Bao, M., Wang, C., Ren, W., Xu, J., 2018b. Ocean acidification and nutrient limitation synergistically reduce growth and photosynthetic performances of a green tide alga *Ulva linza*. Biogeosciences 15, 3409–3420.
Gao, G., Clare, A.S., Rose, C., Caldwell, G.S., 2017a. Eutrophication and warming-driven green tides (*Ulva rigida*) are predicted to increase under future climate change scenarios. Mar. Pollut. Bull. 114, 439–447.
Gao, G., Clare, A.S., Rose, C., Caldwell, G.S., 2017b. Intrinsic and extrinsic control of reproduction in the green tide-forming alga, *Ulva rigida*. Environ. Exp. Bot. 139, 14–22.
Gao, G., Clare, A.S., Rose, C., Caldwell, G.S., 2018c. *Ulva rigida* in the future ocean: potential for carbon capture, bioremediation and biomethane production. GCB Bioenergy 10, 39–51.
Gao, G., Gao, Q., Bao, M., Xu, J., Li, X., 2019. Nitrogen availability modulates the effects of ocean acidification on biomass yield and food quality of a marine crop *Pyropia yezoensis*. Food Chem. 271, 623–629.
Gao, G., Xia, J., Yu, J., Zeng, X., 2018a. Physiological response of a red tide alga (*Skeletonema costatum*) to nitrate enrichment, with special reference to inorganic carbon acquisition. Mar. Environ. Res. 133, 15–23.
Gao, G., Zhao, X., Jiang, M., Gao, L., 2021. Impacts of marine heatwaves on algal structure and carbon sequestration in conjunction with ocean warming and acidification. Front. Mar. Sci. 8, 324–341.
Gao, S., Chen, X., Yi, Q., Wang, G., Pan, G., Lin, A., Peng, G., 2010. A strategy for the proliferation of *Ulva prolifera*, main causative species of green tides, with formation of sporangia by fragmentation. PLoS One 5, e8571.
Gordillo, F.J.L., Jiménez, C., Goutx, M., Niell, X., 2001. Effects of CO_2 and nitrogen supply on the biochemical composition of *Ulva rigida* with especial emphasis on lipid class analysis. J. Plant Physiol. 158, 367–373.
Gouvêa, L.P., Assis, J., Gurgel, C.F., Serrão, E.A., Silveira, T.C., Santos, R., Duarte, C.M., Peres, L.M., Carvalho, V.F., Batista, M., Bastos, E., 2020. Golden carbon of *Sargassum* forests revealed as an opportunity for climate change mitigation. Sci. Total Environ. 729, 138745.
Gouvêa, L.P., Schubert, N., Martins, C.D.L., Sissini, M., Ramlov, F., Rodrigues, E.R.D.O., Bastos, E.O., Freire, V.C., Maraschin, M., Carlos Simonassi, J., Varela, D.A., 2017. Interactive effects of marine heatwaves and eutrophication on the ecophysiology of a widespread and ecologically important macroalga. Limnol. Oceanogr. 62, 2056–2075.
Hobday, A.J., Alexander, L.V., Perkins, S.E., Smale, D.A., Straub, S.C., Oliver, E.C.J., Benthuysen, J.A., Burrows, M.T., Donat, M.G., Feng, M., Holbrook, N.J., Moore, P.J.,

Scannell, H.A., Sen Gupta, A., Wernberg, T., 2016. A hierarchical approach to defining marine heatwaves. Prog. Oceanogr. 141, 227–238.
Holbrook, N.J., Sen Gupta, A., Oliver, E.C.J., Hobday, A.J., Benthuysen, J.A., Scannell, H.A., Smale, D.A., Wernberg, T., 2020. Keeping pace with marine heatwaves. Nat. Rev. Earth Environ. 1, 482–493.
Holdt, S.L., Kraan, S., 2011. Bioactive compounds in seaweed: functional food applications and legislation. J. Appl. Phycol. 23, 543–597.
Huo, Y., Kim, J.K., Yarish, C., Augyte, S., He, P., 2021. Responses of the germination and growth of *Ulva prolifera* parthenogametes, the causative species of green tides, to gradients of temperature and light. Aquat. Bot. 170, 103343.
Keselman, J.C., Lix, L.M., Keselman, H.J., 1996. The analysis of repeated measurements: a quantitative research synthesis. Br. J. Math. Stat. Psychol. 49, 275–298.
Kim, Se-Kwon, 2011. Marine medicinal foods: implications and applications, macro and microalgae (physical, chemical, and biological properties of wonder kelp—*Laminaria*). Adv. Food Nutr. Res. 65, 85–96.
Krause-Jensen, D., Marba, N., Sanz-Martin, M., Hendriks, I.E., Thyrring, J., Carstensen, J., 2016. Long photoperiods sustain high pH in arctic kelp forests. Sci. Adv. 2, e1501938.
Kumari, P., Kumar, M., Reddy, C.R.K., Jha, B., 2014. Nitrate and phosphate regimes induced lipidomic and biochemical changes in the intertidal macroalga *Ulva lactuca* (Ulvophyceae, Chlorophyta). Plant Cell Physiol. 55, 52–63.
Langmead, B., Salzberg, S.L., 2012. Fast gapped-read alignment with bowtie 2. Nat. Methods 9, 357–359.
Li, Y., Ren, G., Wang, Q., You, Q., 2019. More extreme marine heatwaves in the China seas during the global warming hiatus. Environ. Res. Lett. 14, 104010.
Lomstein, B.A., Guldberg, L.B., Neubauer, A.-T.A., Hansen, J., Donnelly, A., Herbert, R.A., Viaroli, P., Giordani, G., Azzoni, R., de Wit, R., Finster, K., 2006. Benthic decomposition of Ulva lactuca: a controlled laboratory experiment. Aquat. Bot. 85, 271–281.
Ma, C., Qin, S., Cui, H., Liu, Z., Zhuang, L., Wang, Y., Zhong, Z., 2021. Nitrogen enrichment mediates the effects of high temperature on the growth, photosynthesis, and biochemical constituents of *Gracilaria blodgettii* and *Gracilaria lemaneiformis*. Environ. Sci. Pollut. Res. 28, 21256–21265.
Ma, Y.Y., Zhao, J., Xie, W.F., Jiang, P., 2020. Branching phenotype and plasticity of the floating ecotype of *Ulva prolifera*. Ocean Sci. 44, 98–105.
McPherson, M.L., Finger, D., Houskeeper, H.F., Bell, T.W., Kudela, R.M., 2021. Large-scale shift in the structure of a kelp forest ecosystem co-occurs with an epizootic and marine heatwave. Commun. Biol. 4, 1–9.
Mi, P., Sui, Z.H., Que, Z., Zhou, W., Shang, E.L., 2017. Microscopic observation of the reproductive development of gametophyte and tetrasporohyte of *Gracilariopsis lemaneiformis* (Rhodophyta). Haiyang Xuebao 39, 99–114.
Nelson, S.G., Glenn, E.P., Conn, J., Moore, D., Walsh, T., Akutagawa, M., 2001. Cultivation of *Gracilaria parvispora* (Rhodophyta) in shrimp-farm effluent ditches and floating cages in Hawaii: a two-phase polyculture system. Aquaculture 193, 239–248.
Nepper-Davidsen, J., Andersen, D.T., Pedersen, M.F., 2019. Exposure to simulated heatwave scenarios causes long-term reductions in performance in saccharina latissima. Mar. Ecol. Prog. Ser. 630, 25–39.
Oliveira, M.C., Ragan, M.A., 1994. Variant forms of a group i intron in nuclear small-subunit rRNA genes of the marine red alga *Porphyra spiralis* var. Amplifolia. Mol. Biol. Evol. 11, 195–207.
Oliver, E.C.J., Burrows, M.T., Donat, M.G., Sen Gupta, A., Alexander, L.V., Perkins-Kirkpatrick, S.E., Benthuysen, J.A., Hobday, A.J., Holbrook, N.J., Moore, P.J., Thomsen, M.S., Wernberg, T., Smale, D.A., 2019. Projected marine heatwaves in the 21st century and the potential for ecological impact. Front. Mar. Sci. 6, 734.
Oliver, E.C.J., Donat, M.G., Burrows, M.T., Moore, P.J., Smale, D.A., Alexander, L.V., Benthuysen, J.A., Feng, M., Sen Gupta, A., Hobday, A.J., Holbrook, N.J., Perkins-Kirkpatrick, S.E., Scannell, H.A., Straub, S.C., Wernberg, T., 2018. Longer and more frequent marine heatwaves over the past century. Nat. Commun. 9, 1324.
Radecker, N., Pogoreutz, C., Gegner, H.M., Cardenas, A., Roth, F., Bougoure, J., Guagliardo, P., Wild, C., Pernice, M., Raina, J.B., Meibom, A., Voolstra, C.R., 2021. Heat stress destabilizes symbiotic nutrient cycling in corals. Proc. Natl. Acad. Sci. U. S. A. 118, e2022653118.
Park, J., 2020. Photosynthetic and biochemical traits change in the green-tide-forming macroalga *Ulva Pertusa* during sporulation. J. Phycol. 56, 549–557.
Rendina, F., Bouchet, P.J., Appolloni, L., Russo, G.F., Sandulli, R., Kolzenburg, R., Putra, A., Ragazzola, F., 2019. Physiological response of the coralline alga *Corallina officinalis* L. to both predicted long-term increases in temperature and short-term heatwave events. Mar. Environ. Res. 150, 104764.
Peredo, E.L., Cardon, Z.G., 2020. Shared up-regulation and contrasting down-regulation of gene expression distinguish desiccation-tolerant from intolerant green algae. Proc. Natl. Acad. Sci. U. S. A. 117, 17438–17445.
Roleda, M.Y., Hurd, C.L., 2019. Seaweed nutrient physiology: application of concepts to aquaculture and bioremediation. Phycologia 58, 552–562.
Smale, D.A., 2019. Impacts of ocean warming on kelp forest ecosystems. New Phytol. 225, 1447–1454.
Smale, D.A., Burrows, M.T., Moore, P., O'Connor, N., Hawkins, S.J., 2013. Threats and knowledge gaps for ecosystem services provided by kelp forests: a Northeast Atlantic perspective. Ecol. Evol. 3, 4016–4038.
Smetacek, V., Zingone, A., 2013. Green and golden seaweed tides on the rise. Nature 504, 84–88.
Sogard, S.M., Able, K.W., 1991. A comparison of eelgrass, sea lettuce macroalgae, and marsh creeks as habitats for epibenthic fishes and decapods. Estuar. Coast. Shelf Sci. 33, 501–519.
Steneck, R.S., Graham, M.H., Bourque, B.J., Corbett, D., Erlandson, J.M., Estes, J.A., Tegner, M.J., 2003. Kelp forest ecosystems: biodiversity, stability, resilience and future. Environ. Conserv. 29, 436–459.
Sambhwani, K., Mathukiya, G., Dawange, P.S., Sequeira, R.A., Prasad, K., Mantri, V.A., 2022. Analysis of functional traits in *Gracilaria dura* (Rhodophyta: Gracilariacae) reveals variation in wild and farmed populations. J. Appl. Phycol. 34, 1017–1031.
Tan, L., Xu, W., He, X., Wang, J., 2019. The feasibility of Fv/Fm on judging nutrient limitation of marine algae through indoor simulation and in situ experiment. Estuar. Coast. Shelf Sci. 229 106411.1-106411.8.
Thomsen, M.S., Mondardini, L., Alestra, T., Gerrity, S., Tait, L., South, P.M., Lilley, S.A., Schiel, D.R., 2019. Local extinction of bull kelp (*Durvillaea* spp.) due to a marine heatwave. Front. Mar. Sci. 6, 1–10.
Torres, P., Santos, J.P., Chow, F., dos Santos, D.Y.A.C., 2019. A comprehensive review of traditional uses, bioactivity potential, and chemical diversity of the genus *Gracilaria* (Gracilariales, Rhodophyta). Algal Res. 37, 288–306.
Traugott, A., Mz, B., Hc, A., Ac, B., Al, A., Ag, B., 2020. Aeration and nitrogen modulated growth rate and chemical composition of green macroalgae *Ulva* sp. Cultured in a photobioreactor. Algal Res. 47, 101808.
Tyler, A.C., Mcglathery, K.J., Macko, S.A., 2005. Uptake of urea and amino acids by the macroalgae *Ulva lactuca* (Chlorophyta) and *Gracilaria vermiculophylla* (Rhodophyta). Mar. Ecol. Prog. Ser. 294, 161–172.
Vanacker, H., 2000. Early H_2O_2 accumulation in mesophyll cells leads to induction of glutathione during the hyper-sensitive response in the barley-powdery mildew interaction. Plant Physiol. 123, 1289–1300.
Wang, B., Wu, L., 2021. Numerical study on the massive outbreak of the *Ulva prolifera* green tides in the southwestern Yellow Sea in 2021. J. Mar. Sci. Eng. 9, 1167.
Wang, H., Lin, A., Gu, W., Huan, L., Gao, S., Wang, G., 2016. The sporulation of the green alga *Ulva prolifera* is controlled by changes in photosynthetic electron transport chain. Sci. Rep. 6, 1–9.
Wernberg, T., Bennett, S., Babcock, R.C., Bettignies, T.D., Cure, K., Depczynski, M., 2016. Climate-driven regime shift of a temperate marine ecosystem. Science 353, 169–172.
Wernberg, T., Smale, D.A., Tuya, F., Thomsen, M.S., Langlois, T.J., Bettignies, T., 2013. An extreme climatic event alters marine ecosystem structure in a global biodiversity hotspot. Nat. Clim. Chang. 3, 78–82.
Wernberg, T., Thomsen, M.S., Tuya, F., Kendrick, G.A., Staehr, P.A., Toohey, B.D., 2010. Decreasing resilience of kelp beds along a latitudinal temperature gradient: potential implications for a warmer future. Ecol. Lett. 13, 685–694.
Werner, F.J., Graiff, A., Matthiessen, B., 2016. Even moderate nutrient enrichment negatively adds up to global climate change effects on a habitat-forming seaweed system. Limnol. Oceanogr. 61, 1891–1899.
Winters, G., Nelle, P., Fricke, B., Rauch, G., Reusch, T.B.H., 2011. Effects of a simulated heat wave on photophysiology and gene expression of high- and low-latitude populations of *Zostera marina*. Mar. Ecol. Prog. Ser. 435, 83–95.
Yang, S.S., Gao, J.F., 2001. Reactive oxygen species, free radicals and plant senescence. J. Northwest Univ. 2, 36–41.
Yao, Y.L., Wang, J.J., Yin, J.J., Zou, X.Q., 2020. Marine heatwaves in China's marginal seas and adjacent offshore waters: past, present, and future. J. Geophys. Res.-Oceans 125, e2019JC015801.
Ye, N., Wang, H., Wang, G., 2006. Formation and early development of tetraspores of *Gracilaria lemaneiformis* (Gracilaria, Gracilariaceae) under laboratory conditions. Aquaculture 254, 219–226.
Zhang, Y., He, P., Li, H., Li, G., Liu, J., Jiao, F., Zhang, J., Huo, Y., Shi, X., Su, R., Ye, N., 2019. *Ulva prolifera* green-tide outbreaks and their environmental impact in the Yellow Sea, China. Natl. Sci. Rev. 6, 825–838.
Zhou, W., Wu, H., Huang, J., Wang, J., Zhen, W., Wang, J., Ni, J., Xu, J., 2022. Elevated-CO_2 and nutrient limitation synergistically reduce the growth and photosynthetic performances of a commercial macroalga *Gracilariopsis lemaneiformis*. Aquaculture 550, 737878.
Zhou, W., Sui, Z., Wang, J., Hu, Y., Kang, K.H., Kim, H.B., Niaz, Z., 2016. Mass cultivation of economically important red alga *Gracilariopsis lemaneiformis* (Gracilariaceae, Rhodophyta) from tetraspores and carpospores. Aquaculture 460, 25–31.